Duplicated Prostate Artery Central Gland Blood Supply: A Retrospective Analysis and Classification System

John S. DeMeritt, MD, Ethan Wajswol, BS, Anoop Wattamwar, MD, Andrew Osiason, MD, Tanya Chervoni-Knapp, NP, and Stacy Zamudio, PhD

ABSTRACT

Angiograms and cone-beam computed tomography scans of 36 consecutive prostate artery embolization patients (72 hemipelves) between October 2014 and February 2018 were reviewed. The hemipelves were classified according to the presence of dual central gland (CG) blood supply and the pattern of vascularization: Type 1 with a single CG blood supply (83.3%; n = 60); Type 2 with 2 independent CG arteries with overlapping territories (9.7%; n = 7); and Type 3 with 2 independent CG arteries with isolated territories (7%; n = 5). Up to 20% of pelvic sides may have more than 1 independent CG prostate artery that should be searched for during prostate artery embolization.

ABBREVIATIONS

BPH = benign prostatic hyperplasia, CG = central gland, IPA = internal pudendal artery, PAE = prostate artery embolization, PZ = peripheral zone

Selective prostate artery embolization (PAE) for the treatment of symptomatic benign prostatic hyperplasia (BPH) was first described by DeMeritt et al in 2000 (1). Several large review articles and meta-analyses have shown PAE to be both safe and effective, resulting in increases in quality of life measures, peak urinary flow rate, post-void residual volume, and an improved International Prostate Symptom Score (2–5). The increasing popularity of PAE requires that radiologists have a sound understanding of the normal pelvic arterial anatomy and its variations, especially given the high variability of prostatic arterial origins (6,7). The superior prostatic pedicle, as described by Garcia-Monaco et al (8), is classically described as consisting of 2 divisions: the medial branch, also called "the artery of adenoma" (9), and the lateral prostatic branch, also called the "capsular branch." The medial prostatic branch primarily supplies the superior and central portion of the prostate gland (the central gland [CG]), while the lateral prostatic branch primarily supplies the peripheral zone (PZ) and apex (10). Herein, the medial prostatic branch will be referred to as the CG branch, and the lateral branch will be referred to as the PZ branch. Complete embolization of the CG blood supply is arguably critical for treating BPH (9,11).

A 2014 cadaveric series revealed that a dual CG blood supply was present in 5.6% of hemipelves (8). In these specimens, 3 pedicles on each side of a hemipelvis were noted: 2 medial prostatic branches originating from the genito-vesical artery and from the middle rectal artery respectively, both supplying the CG, and a single lateral prostatic branch feeding the peripheral zone and prostatic apex, anastomosing with the inferior plexus. In their article, Garcia-Monaco et al questioned what the clinical and technical importance could be when more than 1 pedicle supplies the medial lobe or the CG. This current study attempts to answer the question raised by Garcia-Monaco et al and elucidate the clinical and technical implications

From the Department of Radiology (J.S.D., A.W., A.O., T.C.-K., S.Z), Hackensack University Medical Center, 30 Prospect Avenue, Hackensack, NJ 07601; and Rutgers New Jersey Medical School (E.W.), Newark, New Jersey.
Received April 26, 2018; final revision received July 14, 2018; accepted July 15, 2018.
Address correspondence to J.S.D.; E-mail: jsdermeritt@aol.com; Twitter handle: @jdemeritt

From the SIR 2017 Annual Scientific Meeting.

Appendix A and Figures E1–E10 can be found by accessing the online version of this article on *www.jvir.org* and clicking on the Supplemental Material tab.

J Vasc Interv Radiol 2018; 29:1595–1600

https://doi.org/10.1016/j.jvir.2018.07.010

of this anatomic observation. Reported within is a series of 36 PAE patients, some demonstrating a dual CG blood supply and a classification scheme of their anatomic and hemodynamic subtypes.

MATERIALS AND METHODS

This retrospective review of findings from PAE was approved by the authors' institutional review board. The results of angiograms and cone-beam computed tomography (CT) scans of patients who underwent PAE for symptomatic BPH and/or bleeding of prostate origin between October 2014 and February 2018 were reviewed. Thirty-six patients (comprising 72 hemipelves) were identified as having undergone PAE. Age of the patients, prostate size, and indications for the PAE are listed in Table 1. All patients received a computed tomography angiogram of the pelvis for preprocedural planning purposes. The study was performed on a 64-slice scanner (Siemens Medical Solutions, Munich, Germany) with a 125-mL bolus of ioversol (Optiray 350; Guerbet, Villepinte, France) injected at 4–5 mL/s. Imaging was initiated when a region of interest in the abdominal aorta reached a threshold of 200 HU. Additional scanning parameters included 0.75-mm collimator with reconstructions at 2 mm, pitch of 0.9, 0.5-s gantry rotation period, 100–140 kV, and 95 mA reference with automated modulation along the z-axis based on body mass (CARE Dose 4D; Siemens).

All procedures were performed in a dedicated angiography suite equipped with a floor-mounted fluoroscopy unit (Artis Zeego, Siemens Medical Solutions). Digital subtraction angiography of the right and left anterior divisions of the iliac arteries was performed with an ipsilateral anterior oblique (30 degrees) projection to determine arterial supply to the prostate. In each case, a 1.9F Echelon 10 microcatheter (Medtronic, Minneapolis, Minnesota) was placed into each prostate artery branch supplying the CG of the prostate, as confirmed by cone-beam CT angiography, and distal to any branches with extra-prostatic supply.

All intraprocedural volumetric CT acquisitions were performed once an Echelon 10 microcatheter had been positioned within the prostate artery. Immediately after a 3–5-cc hand injection of undiluted iodinated contrast medium (Isovue 300; Bracco Diagnostic Inc, Monroe Township, New Jersey), a 6-s cone-beam computed tomography angiogram (DynaCT, Siemens Medical Solutions; frame rate: 66.67 fps, kVp: 90-125, FOV: 18.5-cm height x 24-cm diameter, matrix size: 512 x 512) was performed. The projections were automatically transferred to a dedicated interventional workstation performing cone-beam CT reconstruction and displaying the volumetric data for further 3-dimensional analyses. PAE and intraprocedural angiography were performed by a single operator (J.D.) with more than 25 years of experience as an interventional radiologist. To confirm CG or PZ involvement on cone-beam CT, images were reviewed alongside a fellowship-boarded abdominal radiologist with more than 20 years of experience in prostate magnetic resonance interpretation. For the PAE itself, an Echelon 10 1.8-F microcatheter was used to select the prostatic arteries and inject particles. Up to 1 mg of intraarterial verapamil was administered on each pelvic side prior to embolization. Patients were embolized with tris-acryl gelatin microspheres (Embospheres, Merit Medical Systems Inc, South Jordan, Utah) ranging from 100 to 500 microns, and additionally coils were used in 11 patients. The cases were reviewed for the presence of dual CG blood supply and categorized by anatomic subtype.

Table 1. Baseline Patient Characteristics

Number of Patients/Hemipelves	36 (72)
Average Age	70.1 ± 8.2
Average Prostate Size (g)	110.3 ± 72
Indication for PAE	
Symptomatic BPH	23
BPH with Hematuria	6
Status Post TURP with Hematuria	4
Prostate Cancer with Hematuria	2
Radiation Prostatitis with Hematuria	1

BPH = benign prostatic hyperplasia; PAE = prostate artery embolization; TURP = transurethral resection of the prostate.

Anatomic subtypes were divided into 4 distinct categories, each representing a distinct pattern of dual prostate artery blood supply and vascularization. Type 1A was defined as the classic pattern in which a single main prostate artery divides into CG and PZ branches. Type 1B was defined as a variant of the classic pattern with 2 separate prostate arteries or pedicles, one feeding the CG and the other feeding the PZ. Type 2 was defined as at least 2 communicating or overlapping prostate pedicles supplying a single vascular compartment encompassing the entire CG (± a separate PZ pedicle). Type 3 was defined as at least 2 independent noncommunicating prostate pedicles each supplying a portion or fraction of the CG, constituting multiple isolated vascular compartments (± a separate PZ pedicle). Types 1 and 2 both reflect a single CG vascular compartment, differing only in the number of CG pedicles. The classification system allows for the possibility of an independent PZ pedicle and supplied territory in Types 2 and 3, represented by ±. A visual representation of the classification system is depicted is Figure 1.

RESULTS

Type 1A prostatic vascularization was identified in 57 hemipelves (79.2%), Type 1B in 3 hemipelves (4.2%), Type 2 in 7 hemipelves (9.7%), and Type 3 in 5 hemipelves (6.9%). The overall distribution of hemipelves by classification type is summarized in Table 2. Dual CG blood supply, defined as duplication of the medial prostatic branch arteries, was identified in 12 pelvic sides (16.7%) overall, irrespective of the prostatic compartmentalization pattern. When duplicated

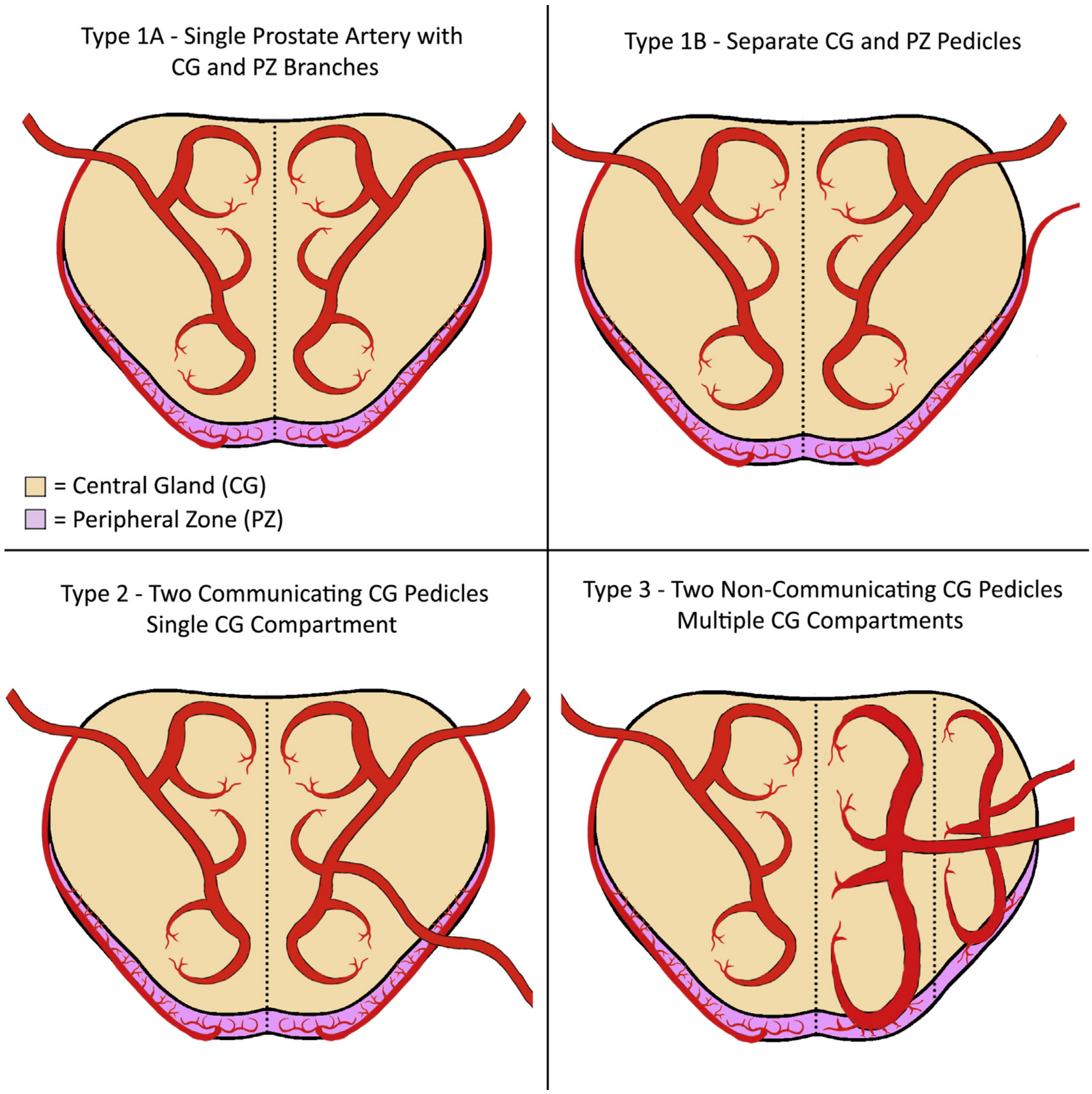

Figure 1. Visual coronal plane representation of prostatic arterial classification system. The left hemiprostate in each example is the portion of the prostate demonstrating the subtype. Note that Types 1 and 2 both reflect a single CG vascular compartment, only differing in the number of CG pedicles. Type 3 reflects multiple CG vascular compartments with corresponding multiple noncommunicating CG vascular pedicles. In Type 3 vascularization, the classic intraprostatic arborization pattern into medial and lateral branches is not depicted, with split CG and PZ supply conforming to the orientation of their respective vascular compartments. Types 2 and 3 are illustrated without an independent PZ pedicle.

Table 2. Prostatic Vascularization Types

Type 1A—Single Main Prostate Artery	57
Type 1B—Separate CG and PZ Pedicles	3
Type 2—Multiple CG Pedicles with a Single CG Compartment	7
Type 3—Multiple CG Pedicles with Multiple CG Compartments	5

CG = central gland; PZ = peripheral zone.

arteries supplied the CG, their anatomic parent vessel origin was highly variable, with examples observed originating from the obturator artery, internal pudendal artery (IPA), and other anterior division vessels. An example of a Type 2 vascularization pattern with 3 prostate arteries (2 originating from the IPA and 1 dominant feeder from the vesicoprostatic trunk) is depicted in Figure 2. The most commonly observed origination vessel for a duplicated CG pedicle in the context of Type 2 vascularization was the obturator artery, seen in 4 hemipelves. Duplicated CG prostate pedicles were not confined to the same anatomic side of the hemiprostate they supplied. Duplicated arteries in both Type 2 and Type 3 subtypes were found to be either ipsilateral or contralateral relative to the hemiprostate they supplied. In Type 2 vascularization, different degrees of CG opacification were observed from the respective duplicated pedicles based on their relative hemodynamic balance and injection strength. When Type 3 patterns were observed, the spatial orientation and volume of the compartments was variable, with a superior/inferior arrangement, a medial/lateral arrangement, and more complex arrangements. In Type 3 vascularization, the classic intraprostatic arborization pattern into medial and

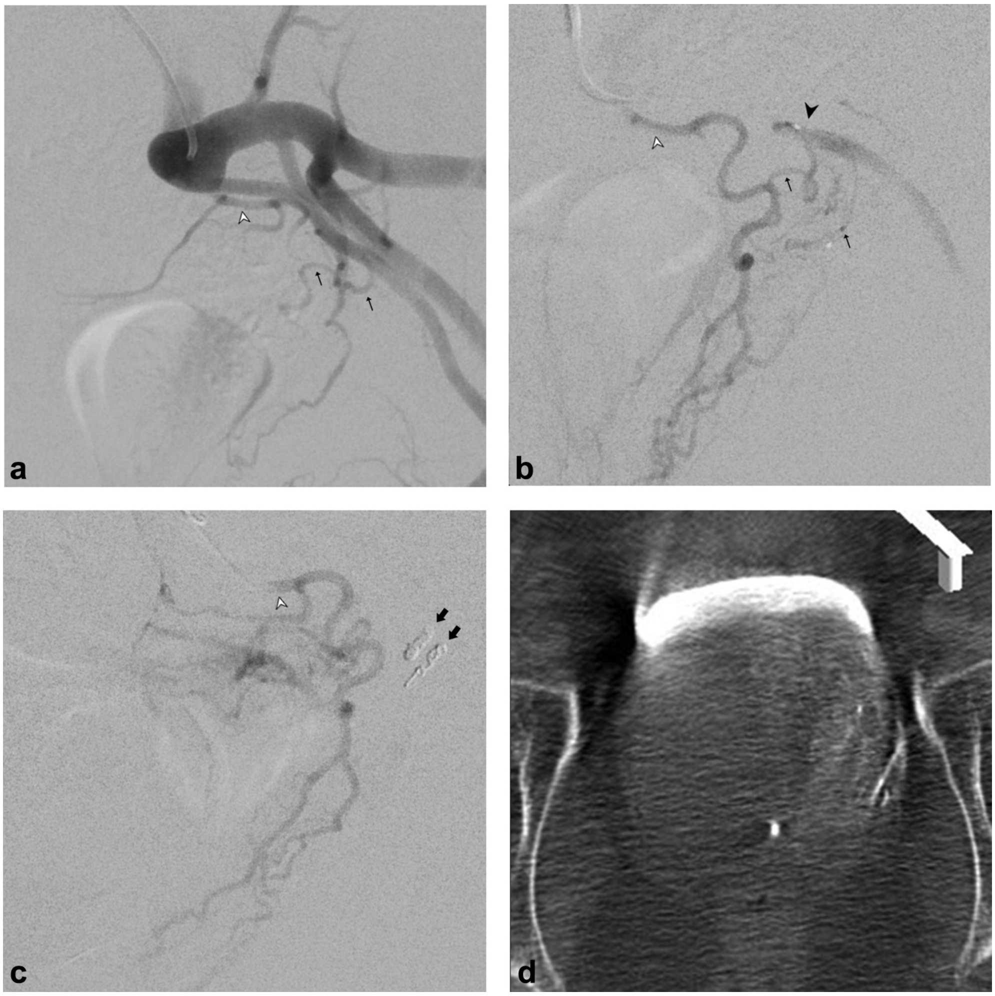

Figure 2. (**a**) Angiography of the internal iliac artery. Note the presence of 3 distinct prostatic pedicles: the prostatic artery arising from the vesicoprostatic trunk (marked by white arrowhead) and 2 separate IPA pedicles (marked by black arrows). (**b**) Angiography after catheterization of the second (distal) IPA prostate pedicle. Note the catheter tip position (black marker bead) inside the distal IPA prostate pedicle. Note retrograde opacification of the vesicoprostatic pedicle and the more proximal IPA pedicle. The vesicoprostatic trunk is marked by a white arrowhead, the IPA by a black arrowhead, and the duplicated IPA prostate pedicles by black arrows. (**c**) Selective angiography of the vesicoprostatic trunk (white arrowhead) originating prostate artery after coil embolization of both IPA prostatic pedicles, with opacification of the left prostate artery territory. Note that there is no retrograde opacification of the IPA. Note the subtraction artifact of coils placed inside each of the occluded IPA pedicles, marked by black arrows. (**d**) Cone-beam CT demonstrating opacification of the left hemigland.

lateral branches was not observed, with split CG and PZ supply arising from the respective pedicles conforming to the observed geometric patterns, as shown in **Figure 1**. An example of a Type 3 pattern displaying a medial and lateral vascular compartment arrangement is depicted in **Figure 3**. In Types 2 and 3, the entire CG and PZ were ultimately supplied by the duplicated pedicles, as shown in **Figure 1**; no cases were seen in which a separate PZ pedicle was identified in these subsets. Additional examples of Type 2 and Type 3 vascularization patterns may be viewed in **Appendix A** and **Figures E1–E10** (available online on the article's Supplemental Material page at *www.jvir.org*).

DISCUSSION

The current study identifies and describes the vascular compartmentalization patterns of dual CG blood supply with 2 distinct subtypes: Type 2 (single vascular compartment) and Type 3 (multiple vascular compartments). One important principle derived from the current study is the need for careful angiographic investigation during PAE to avoid nontarget embolization in the setting of Type 2 anatomy: a single vascular compartment with at least 2 communicating or overlapping CG pedicles. Free communication between 2 pedicles within a shared CG vascular territory could result in retrograde flow in the second vessel, with unwanted nontarget embolization. Cone-beam CT, and perhaps more importantly strong injection strength angiography, can be used to detect nontarget-end organ supply via retrograde flow through unappreciated duplicated CG pedicles in the setting of a singular vascular compartment. Type 2 vascularization also provides the unique opportunity to embolize the gland through an alternative pathway, which may be clinically advantageous. For example, Type 2

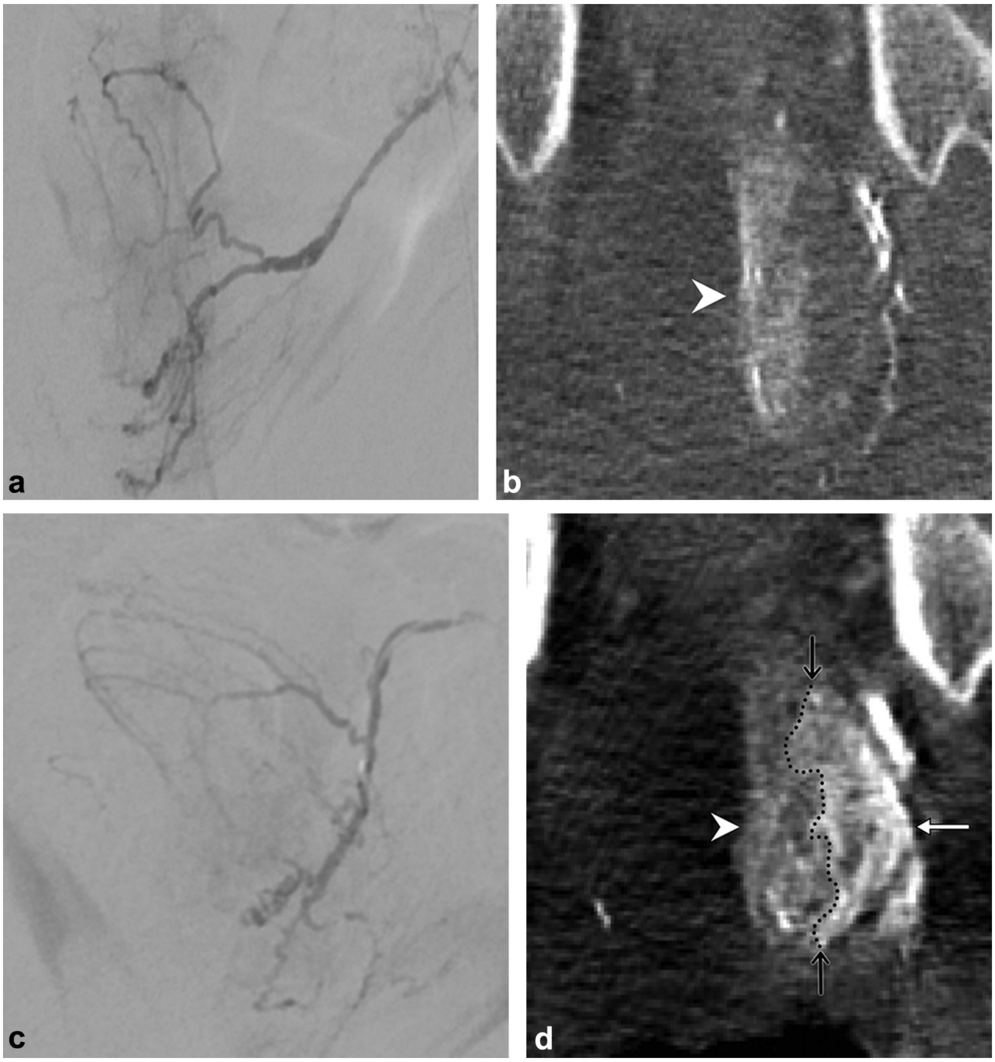

Figure 3. (**a**) Angiography of the left medial CG pedicle supplying the isolated medial vascular compartment. (**b**) Axial cone-beam CT of the opacified isolated left medial prostatic vascular compartment (white arrowhead) supplied by a separate medial CG pedicle. (**c**) Angiography of the left lateral CG pedicle supplying the isolated lateral vascular compartment. (**d**) Axial cone-beam CT of the opacified isolated left lateral prostatic vascular compartment (white arrow) after PAE of the medial CG pedicle. Note retained contrast medium in the medial compartment (white arrowhead) from the immediate prior medial pedicle embolization. A dotted line with the ends marked by black arrows demarcates the opacification of the respective medial and lateral compartments.

vascularization with a contralateral supplying pedicle may allow for embolization of the entire prostate from a single side, saving time. Alternatively, 2 ipsilateral CG pedicles, which freely communicate in the context of a single vascular compartment, provide the opportunity to embolize the hemigland from a second site when the other pedicle is extremely difficult to catheterize, stenotic, or occluded. For example, when the prostate artery arises from the vesicoprostatic trunk, it is often angulated and difficult to catheterize, whereas its origin from the obturator artery is often straight and relatively easy to catheterize, which was the most commonly observed origin of Type 2 dual CG blood supply in the series (n = 4). Competitive inflow from a second CG pedicle in the setting of Type 2 anatomy can also prevent uniform particle distribution, necessitating independent embolization of both pedicles or coil embolization of the undesirable inflow, as was seen in 1 case (shown in **Appendix A** [available online on the article's Supplemental Material page at *www.jvir.org*]).

Type 3 anatomy, consisting of multiple vascular compartments, may have different and unique potential clinical implications. One possible clinical implication is that failure of therapeutic response after PAE could hypothetically be due to a lack of recognition of dual CG blood supply with Type 3 prostatic vascularization. If the interventional radiologist embolizes only 1 isolated vascular compartment when in fact 2 or more exist, a subtherapeutic response may theoretically result. Cone-beam CT is recognized as a useful technique for identifying target versus nontarget vascular supply, as first described by Bagla et al (12). Cone-beam CT was critical for recognizing multiple vascular compartments, which often could not be readily identified from standard angiographic images, particularly when 1 of the compartments was disproportionately small.

In this context, cone-beam CT can be important in ensuring that the entire CG is treated during PAE to potentially maximize therapeutic response. Currently, the estimated rate of failure to induce a long-term clinical effect (after 3 years) after PAE is near 21.9% (13). Although limited data exist, cadaveric data show that the incidence of dual CG blood supply is 5.6% of pelvic sides (8). In the current study, it is estimated that the percentage of pelvic sides with all subtypes of dual CG blood supply was 16.7% (or 27.7% of patients, since it only occurred bilaterally in 2 patients). Specifically, the percentage of pelvic sides with a multiple isolated compartment subtype was approximately 7% of the total. This latter group may account for some proportion of reported treatment failures if the entire CG is not identified and fully embolized. Similar to unilateral PAE, it is reasonable to hypothesize that a failure of recognition of dual CG blood supply with multiple isolated compartments may account for a reduced clinical response after PAE (14). Although speculative, the strategic location of the vascular compartment might also have specific clinical implications. For example, an isolated medial compartment (**Fig 3**) might be more important to embolize based on its proximity to the urethra than a lateral compartment in a patient with bleeding BPH or, for that matter, for urethral decompression in the setting of bladder outlet obstruction.

Limitations of the current study include a small sample size as well as the inherent limitations of retrospective reviews. Additionally, if the entire CG was targeted on cone-beam CT, embolization was proceeded with, and no attempt was made to routinely selectively catheterize and embolize a separate PZ branch. Another limitation was the lack of clinical correlation with variant anatomy. Although contact with patients was maintained after the procedure, and some International Prostate Symptom Score data were available through correspondence, detailed data including peak urinary flow rate, quality of life, post-void residual volume, and International Index of Erectile Dysfunction score were not routinely obtained. Further studies should focus on the clinical outcomes in patients with different compartmentalization patterns.

In conclusion, a clinically relevant vascular classification system is proposed to describe duplicated CG blood supply and to introduce the concept of prostate vascular compartmentalization. Based on the data presented in the current study, it is estimated that the overall percentage of pelvic sides with duplicated CG blood supply is 16.7% (27.7% of patients). Type 2 vascularization (single compartment with multiple communicating CG pedicles) was observed in 9.7% of pelvic sides, allowing for CG embolization from more than 1 approach but also unwanted competitive inflow or nontarget reflux. Type 3 vascularization (multiple isolated compartments with multiple noncommunicating CG pedicles) was observed in 6.9% of pelvic sides, requiring separate embolization of the individual CG pedicles, for which cone-beam CT was critical for recognition.

ACKNOWLEDGMENTS

Special thanks to Alexandra DeMeritt for illustrations.

REFERENCES

1. DeMeritt JS, Elmasri FF, Esposito MP, Rosenberg GS. Relief of benign prostatic hyperplasia-related bladder outlet obstruction after transarterial polyvinyl alcohol prostate embolization. J Vasc Interv Radiol 2000; 11: 767–770.
2. Cizman Z, Isaacson A, Burke C. Short- to midterm safety and efficacy of prostatic artery embolization: a systematic review. J Vasc Interv Radiol 2016; 27:1487–1493.e1.
3. Wang XY, Zong HT, Zhang Y. Efficacy and safety of prostate artery embolization on lower urinary tract symptoms related to benign prostatic hyperplasia: a systematic review and meta-analysis. Clin Interv Aging 2016; 11:1609–1622.
4. Uflacker A, Haskal ZJ, Bilhim T, Patrie J, Huber T, Pisco JM. Meta-analysis of prostatic artery embolization for benign prostatic hyperplasia. J Vasc Interv Radiol 2016; 27:1686–1697.e8.
5. Kuang M, Vu A, Athreya S. A systematic review of prostatic artery embolization in the treatment of symptomatic benign prostatic hyperplasia. Cardiovasc Intervent Radiol 2017; 40:655–663.
6. Bilhim T, Pereira JA, Fernandes L, Tinto HR, Pisco JM. Angiographic anatomy of the male pelvic arteries. AJR Am J Roentgenol 2014; 203: W373–W382.
7. Bilhim T, Pisco JM, Furtado A, et al. Prostatic arterial supply: demonstration by multirow detector angio CT and catheter angiography. Eur Radiol 2011; 21:1119–1126.
8. Garcia-Monaco R, Garategui L, Kizilevsky N, Peralta O, Rodriguez P, Palacios-Jaraquemada J. Human cadaveric specimen study of the prostatic arterial anatomy: implications for arterial embolization. J Vasc Interv Radiol 2014; 25:315–322.
9. Bouissou H, Talazac A. [Arterial vascularization of the normal and the pathological prostate]. Ann Anat Patol (Paris) 1959; 4:63–79.
10. Clegg EJ. The vascular arrangements within the human prostate gland. Br J Urol 1956; 28:428–435.
11. Bilhim T, Pisco JM, Rio Tinto H, et al. Prostatic arterial supply: anatomic and imaging findings relevant for selective arterial embolization. J Vasc Interv Radiol 2012; 23:1403–1415.
12. Bagla S, Rholl KS, Sterling KM, et al. Utility of cone-beam CT imaging in prostatic artery embolization. J Vasc Interv Radiol 2013; 24:1603–1607.
13. Pisco J, Bilhim T, Ribeiro M, Fernandes L, Costa N, Oliveira A. Short-, medium-, and long-term outcome of prostate artery embolization for patients with benign prostatic hyperplasia: 1000 patients. J Vasc Interv Radiol 2017; 28:S3.
14. A Pereira J, Bilhim T, Duarte M, Rio Tinto H, Fernandes L, Martins Pisco J. Patient selection and counseling before prostatic arterial embolization. Tech Vasc Interv Radiol 2012; 15:270–275.

APPENDIX A. TYPE 2 (SINGLE CG COMPARTMENT) SUPPLEMENTAL CASE EXAMPLES

In the first supplemental example of Type 2 anatomy, duplicated ipsilateral pedicles originated from the left internal pudendal artery, with superior and inferior supplying pedicles (Fig E1). In this patient, a dynamic flow pattern was observed within this vascular territory, whereby slow injection of contrast medium into the first pedicle resulted in anterograde flow with no retrograde flow out of the second pedicle. However, when the injection strength was increased, injection of the superior pedicle resulted in retrograde flow in the inferior pedicle and subsequently into the internal pudendal artery territory, indicating an unacceptable risk of nontarget embolization (Figs E1, E2). An attempt was made to coil one of the dual ipsilateral pedicles, but this was unsuccessful. The tortuous nature of the vessel resulted in failure to gain distal purchase. In this case, only contralateral unilateral prostate artery embolization was achieved.

Four other cases displayed Type 2 vascular compartmentalization, with ipsilateral feeders originating from the vesicoprostatic trunk and the obturator, respectively. In the first example of this variant (Fig E3), contrast medium injection in the first pedicle originating from the vesicoprostatic trunk led to retrograde opacification of the second feeding pedicle originating from the obturator artery, demonstrating overlap or communication of the respective vascular territories. The identity of the second feeding CG pedicle was confirmed by distal intraprostatic catheterization via the first CG pedicle originating from the vesicoprostatic trunk with reflux into the more proximal parent obturator artery. The entire hemiprostate was embolized via the duplicated prostate artery originating from the left vesicoprostatic trunk. Anterograde catheterization and embolization of the left obturator feeder was not necessary.

One of the other examples of Type 2 vascular compartmentalization fed by the vesicoprostatic trunk and obturator artery demonstrated a unique hemodynamic pattern during contrast medium injection (Figs E4, E5). Initial angiography of the duplicated prostatic feeder originating from the vesicoprostatic trunk demonstrated competitive inflow with an area of wash-out by un-opacified blood, corresponding to approximately the inferior third of the hemiprostate or CG. Distal advancement of the catheter and forceful injection of contrast medium revealed staining of a portion of previously unseen inferior gland with reflux into a second prostatic feeder. In an attempt to facilitate the anterograde delivery of embolic particles via the CG pedicle originating from the vesicoprostatic trunk, a distal intraprostatic coil was deployed to eliminate the competitive inflow. Repeat angiography demonstrated improved anterograde flow and glandular blush but persistent incomplete staining of the left inferior hemigland confirmed with a subsequent cone-beam CT. After particulate embolization of the CG pedicle originating from the left vesicoprostatic trunk, the duplicated obturator prostatic feeder was independently catheterized in an anterograde fashion, and angiography was performed. A complex pattern of vascular compartmentalization was revealed whereby the duplicated left obturator feeder supplied the inferior aspects of the respective hemiglands. Particulate embolization of the second duplicated left obturator CG pedicle was then independently performed. Although analysis of the pattern was complicated by coil embolization, a mixed pattern of vascular compartmentalization was suspected with Type 2/3 compartmentalization and Type 3 compartmentalization present in the left and right hemiglands, respectively.

The last Type 2 compartmentalization example, depicted in Figure E6, demonstrated contralateral supply, with a transverse CG pedicle that permitted blood flow from left to right as well as a separate ipsilateral right prostate artery. The overlapping single vascular territory allowed for prostate artery flow from left to right via the transverse CG pedicle. During contrast medium injection into the contralateral left transverse pedicle, reflux into the right inferior vesicle artery was seen with strong injection, with subsequent enhancement of bladder tissue confirmed on cone-beam CT (Fig E6). Because of the high risk of nontarget embolization of the bladder due to reflux, the decision was made to coil the contralateral left transverse pedicle in the hopes of ensuring right prostate artery anterograde flow (Fig E7). After coiling the contralateral left transverse pedicle, anterograde right-sided PAE was safely achieved. Separate left-sided PAE preceded catheterization and coiling of the left to right transverse pedicle.

TYPE 3 (MULTIPLE CG COMPARTMENTS) SUPPLEMENTAL CASE EXAMPLES

Several additional examples of Type 3 compartmentalization were identified. One example of a Type 3 compartmentalization case was identified that was supplied by 2 separate ipsilateral anterior division CG pedicles (Fig E8). Cone-beam CT demonstrated an isolated medial compartment as well as an isolated superior and lateral vascular compartment with no territorial overlap, albeit with differing volumes of the respective compartments. Note intense staining of the smaller-volume periurethral or medial compartment in this patient who presented with bleeding BPH.

Another example was identified that similarly was supplied by 2 separate ipsilateral anterior division CG pedicles but with a somewhat different spatial orientation of the respective compartments, namely primarily superior and inferior (Fig E9). Cone-beam CT demonstrated an isolated superolateral compartment as well as an isolated inferomedial vascular compartment with no territorial overlap. The 2 separate compartments were of similar respective volumes.

Another Type 3 case consisted of 2 independent vascular compartments with both ipsilateral supply and a second duplicated contralateral feeding pedicle, displayed in Figures E4g, E5b, and E5c. One of the territories was an isolated right-sided inferior compartment fed by an independent left-sided contralateral CG pedicle. The superior portion of the right prostate was fed by a separate right-sided CG pedicle, constituting a separate independent vascular compartment.

One last example of Type 3 anatomy is displayed in Figure E10, consisting of 2 independent vascular territories with 2 contralateral feeding pedicles. One of the territories was an isolated right-sided inferior compartment fed by an independent left-sided contralateral CG pedicle. The superior portion of the right prostate as well as the entire left hemiprostate were supplied by a separate left-sided CG pedicle, constituting a single vascular compartment. Complete embolization of the entire prostate was accomplished from the left side via the 2 separate CG pedicles supplying both sides of the gland.

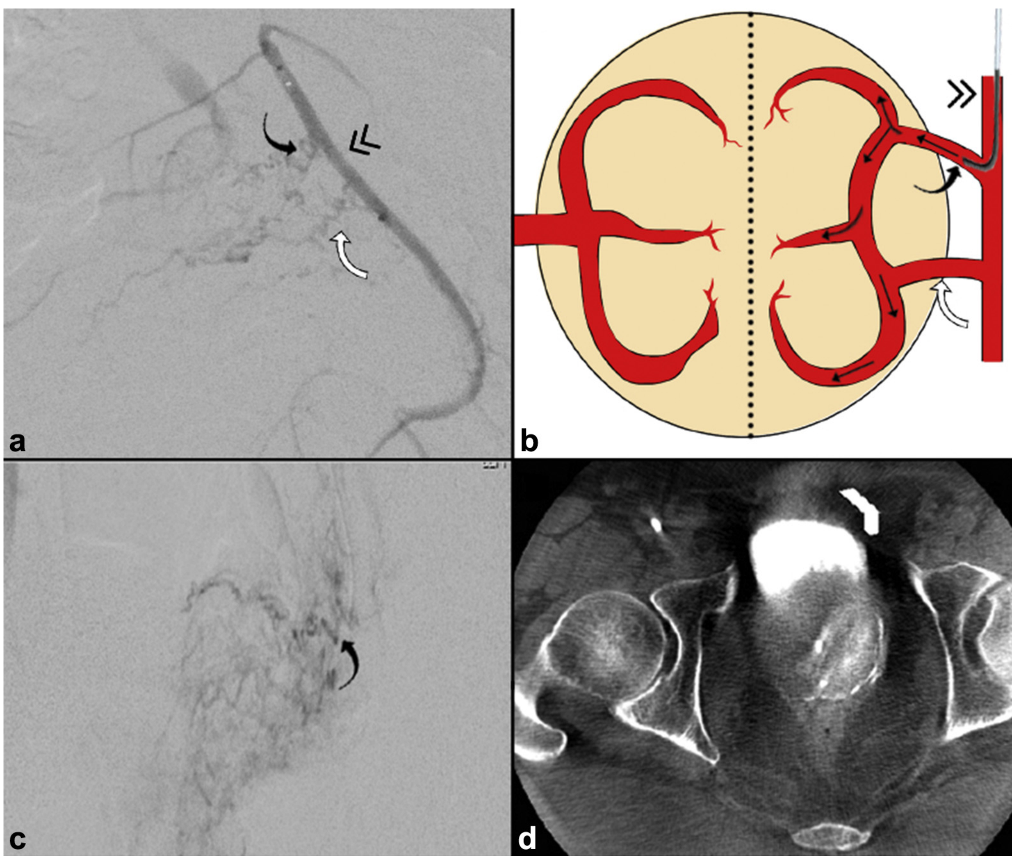

Figure E1. (**a**) Angiography displaying duplicated ipsilateral CG arterial supply stemming from the IPA. Note the superior pedicle (curved black arrow), inferior pedicle (curved white arrow), and IPA, marked by the double arrow heads. (**b**) Schematic representation of Type 2 vascular compartmentalization supplied by ipsilateral feeders with overlapping territories and flow dynamics of a CG pedicle when injected with low strength. Note the arrows indicating the anterograde direction of flow with no reflux into the IPA. (**c**) Angiography of the superior pedicle while being injected with contrast medium with low strength; note the anterograde direction of flow with no reflux from the inferior pedicle. (**d**) Cone-beam CT displaying opacification of the entire left hemiprostate.

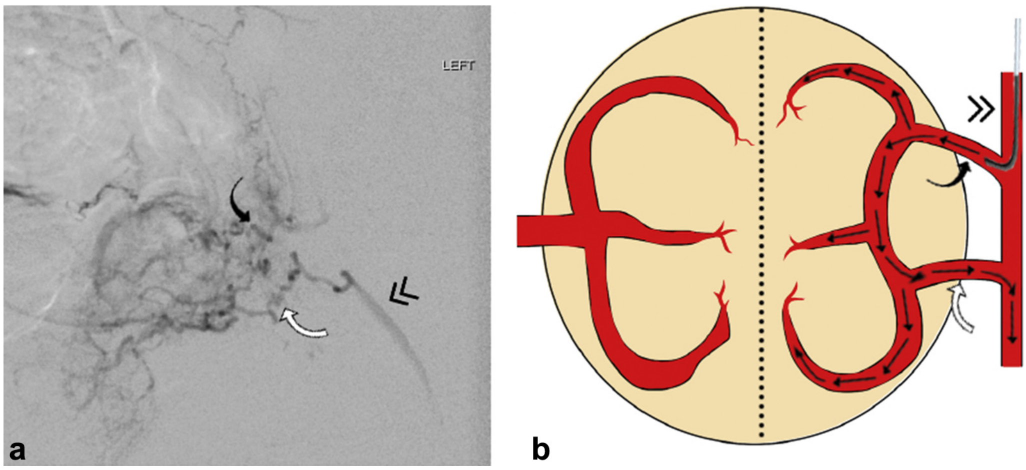

Figure E2. (**a**) Angiography of the duplicated ipsilateral CG arterial supply stemming from the IPA during high injection strength of contrast medium; retrograde flow of contrast medium results in subsequent reflux from the inferior pedicle. Note the superior pedicle (curved black arrow), inferior pedicle (curved white arrow), and IPA, marked by the double arrow heads. (**b**) Diagrammatic representation of the flow dynamics of a Type 2 case with duplicated ipsilateral CG supply originating from the same vessel when injected into the superior pedicle with high strength; note the high rate of contrast medium injection results in retrograde flow into the inferior pedicle and subsequently into the IPA territory, which was not seen with a low injection strength.

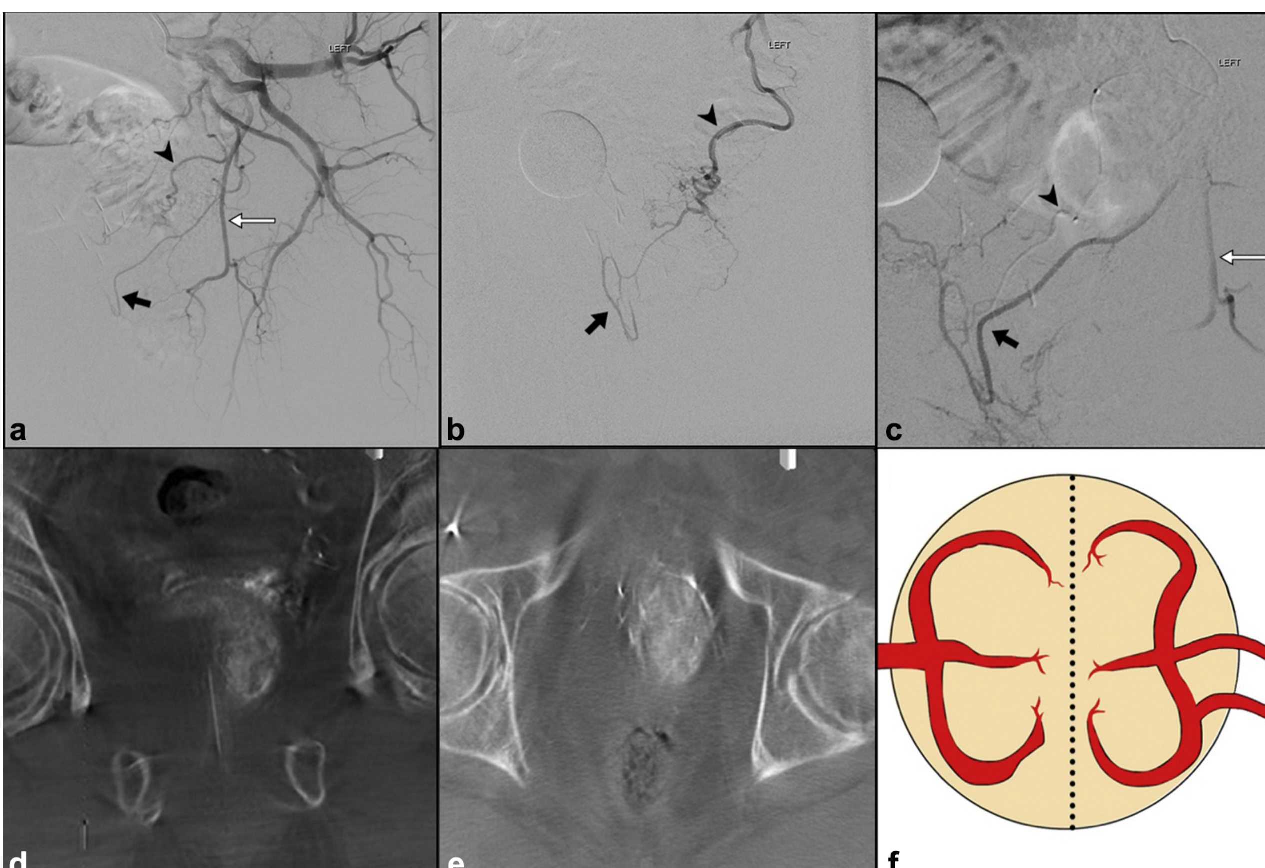

Figure E3. (**a**) Angiography of left internal iliac artery. Note one of the duplicated prostatic pedicles (black arrowhead) originating from the vesicoprostatic trunk and the second duplicated prostatic pedicle (black arrow) originating from the obturator artery (white arrow). (**b**) Angiography after selective catheterization of the first duplicated prostatic pedicle originating from the vesicoprostatic trunk. Retrograde filling of the second duplicated prostatic pedicle originating from the obturator artery can be identified. (**c**) Angiography after further distal advancement of the microcatheter into the first duplicated prostatic pedicle originating from the vesicoprostatic trunk. Note the retrograde filling of the obturator artery confirming the origin of the second duplicated prostatic pedicle. (**d**) Coronal cone-beam CT displaying opacification in the left hemiprostate. (**e**) Axial cone-beam CT displaying opacification of the left hemiprostate (**f**) Line diagram depicting a Type 2 example with 2 separate ipsilateral feeders and overlapping or communicating vascular territories.

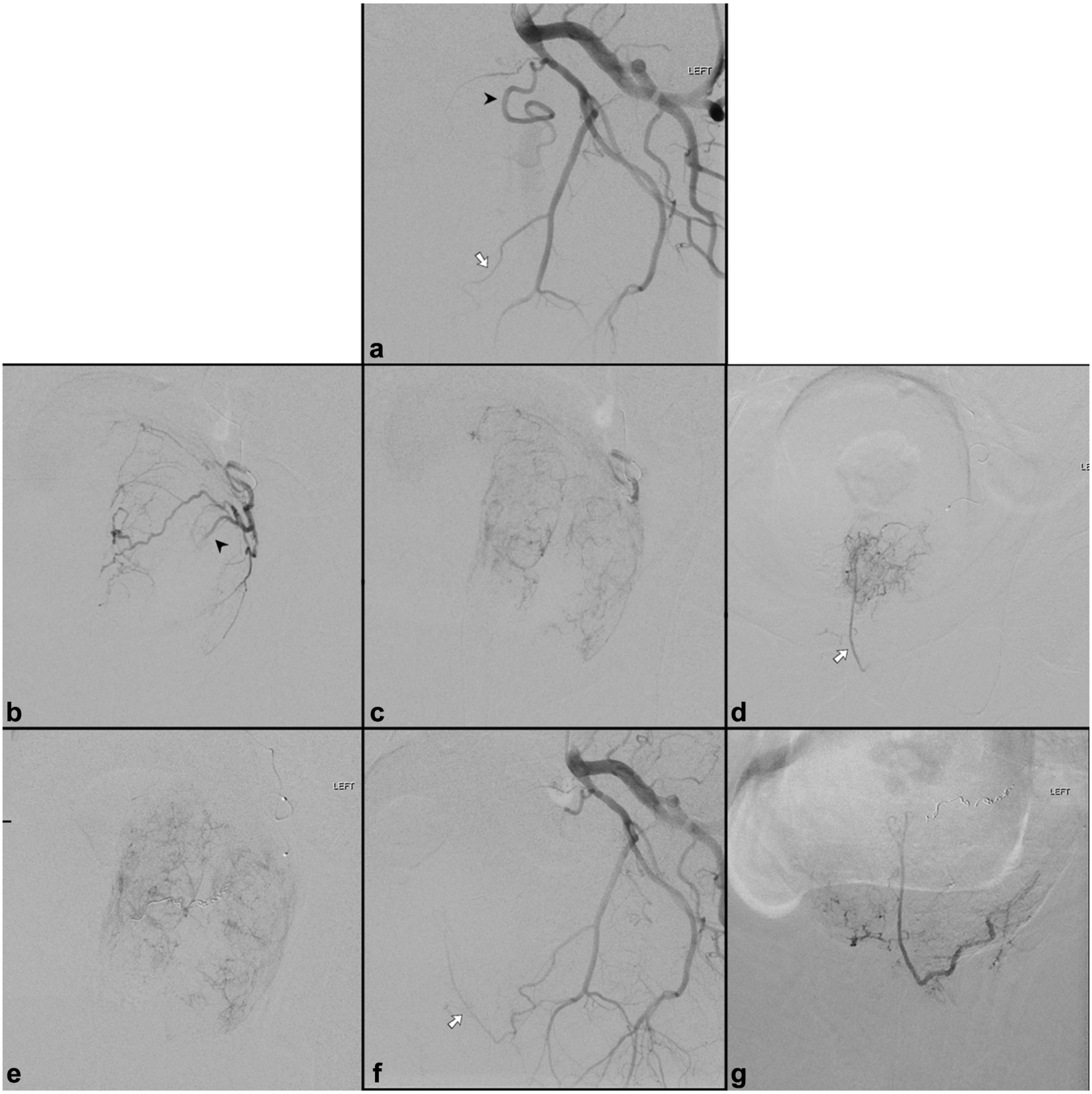

Figure E4. (**a**) Angiography of the internal iliac artery. Both duplicated prostate feeders can be visualized: a superior one originating from the vesicoprostatic trunk (marked by black arrow) and an inferior one originating from the obturator (marked by white arrow). (**b**) Angiography after contrast medium injection within the duplicated vesicoprostatic trunk prostate feeder; note an area of washout (marked by black arrowhead) by inflowing un-opacified blood supplied by the duplicated prostate feeder originating from the obturator artery (**c**) Later phase angiography of (**b**). (**d**) Angiography after further distal catheterization of the vesicoprostatic trunk and forceful injection of contrast medium. Note opacification of before-unseen vascular territory with reflux into the duplicated obturator feeder (marked by white arrow). (**e**) Repeat angiography after coil embolization of the intraprostatic branch with competitive inflow demonstrating improved anterograde flow and glandular blush but persistent incomplete staining of the left inferior hemigland. (**f**) Later-phase angiography of internal iliac artery displaying origin point of the second duplicated prostate feeder (marked by white arrow) stemming from the obturator artery. (**g**) Angiography after selective catheterization of the obturator feeder. Note bilateral branches arising from the duplicated left obturator feeder as it traverses in a midline superior direction, supplying inferior portions of both hemiglands.

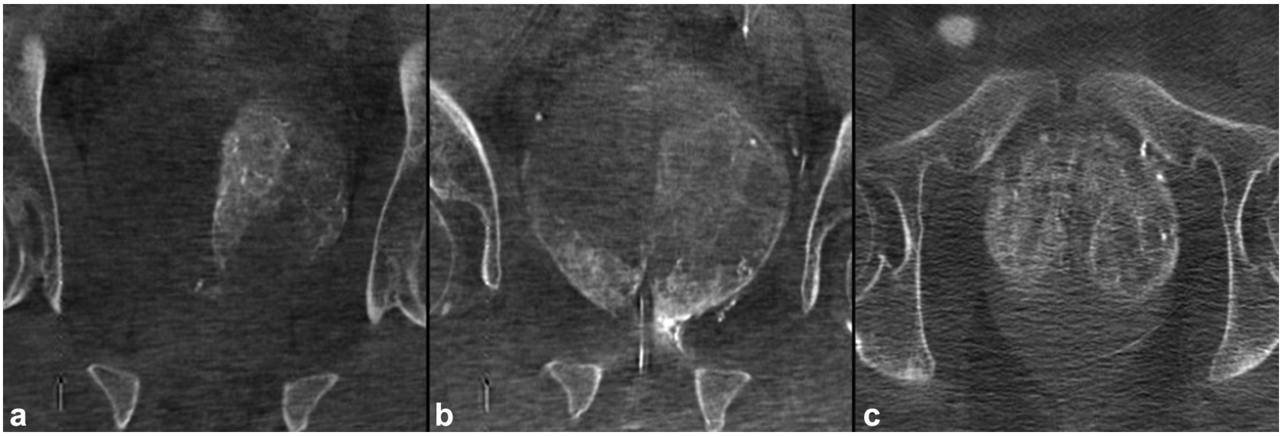

Figure E5. (**a**) Coronal cone-beam CT after contrast medium injection of the duplicated prostatic feeder originating from the vesicoprostatic trunk, after coil embolization of competitive inflow. Note the opacification of the majority of the left hemigland and the relative lack of opacification of the inferior third of the hemigland. (**b**) Coronal cone-beam CT after selective catheterization of the duplicated prostatic feeder originating from the left obturator artery and injection of contrast medium. Note both ipsilateral and contralateral opacification of the inferior portions of the respective hemiglands as well as faint residual staining of the more superior left hemiprostate from immediately prior left vesicoprostatic trunk embolization. Note bilateral inferior hemigland compartmentalization. (**c**) Axial cone-beam CT of (**b**); note the extent of opacification encompassing the bilateral inferior hemiglands or CGs.

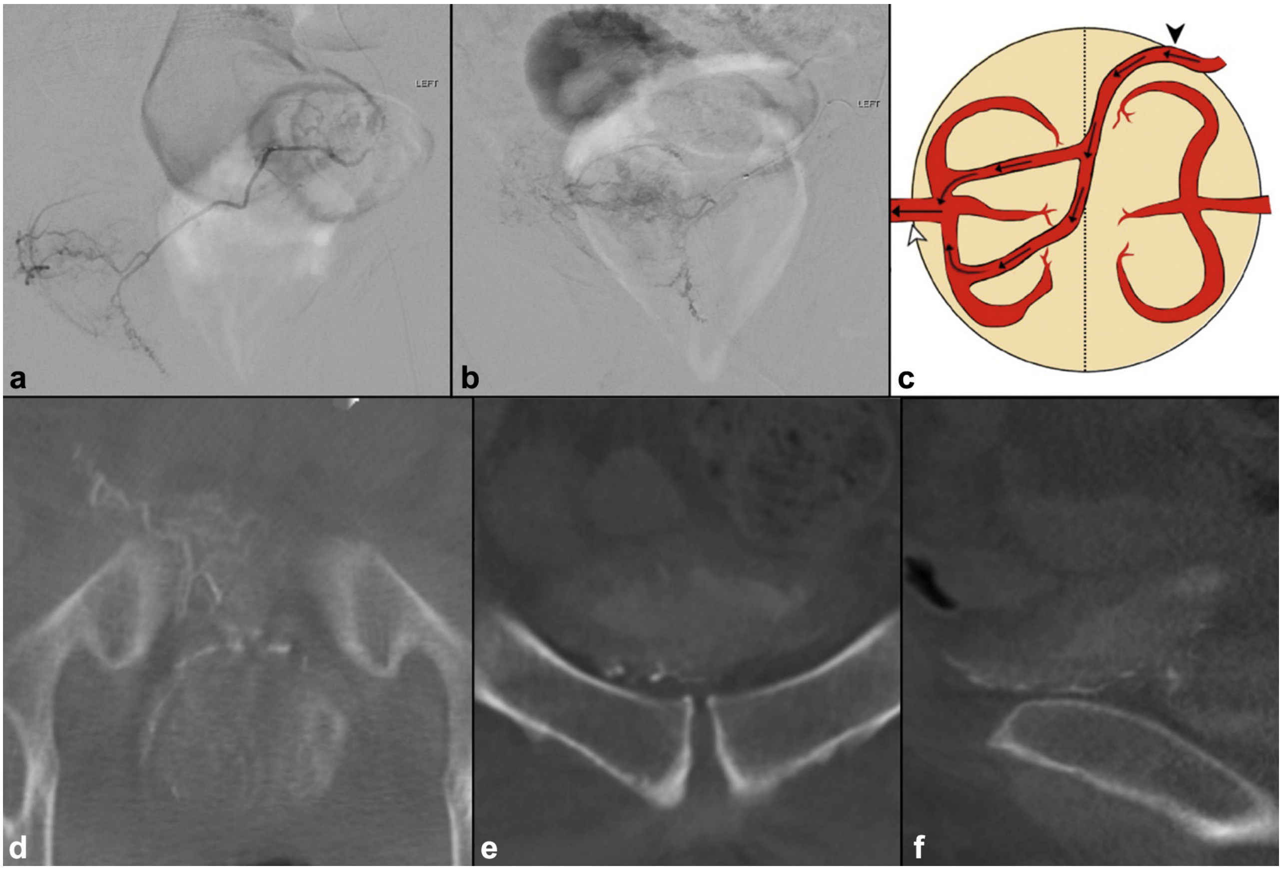

Figure E6. (**a**) Angiography of injection of the left contralateral transverse CG pedicle with opacification of the right-sided intraprostatic vascular plexus. Patency of the right prostate artery was known from preprocedural computed tomography angiography. (**b**) Late-phase angiography of the left transverse CG pedicle depicting reflux into the right inferior vesical artery with staining of the right bladder wall (**c**) Schematic representation of the single vascular compartment dual CG blood supply with contralateral supply, with arrows indicating left to right flow via the left transverse CG pedicle prior to embolization (skinny black arrows). The right prostate artery is depicted by a white arrowhead. (**d**) Axial cone-beam CT displaying staining of the right hemiprostate prior to embolization as well as staining of the right inferior bladder. Residual staining of the left hemiprostate is also evident from immediately prior embolization of the left prostate artery. (**e**) Coronal cone-beam CT displaying staining of the right inferior bladder wall (**f**) Sagittal cone-beam CT images demonstrating staining of the right inferior bladder wall.

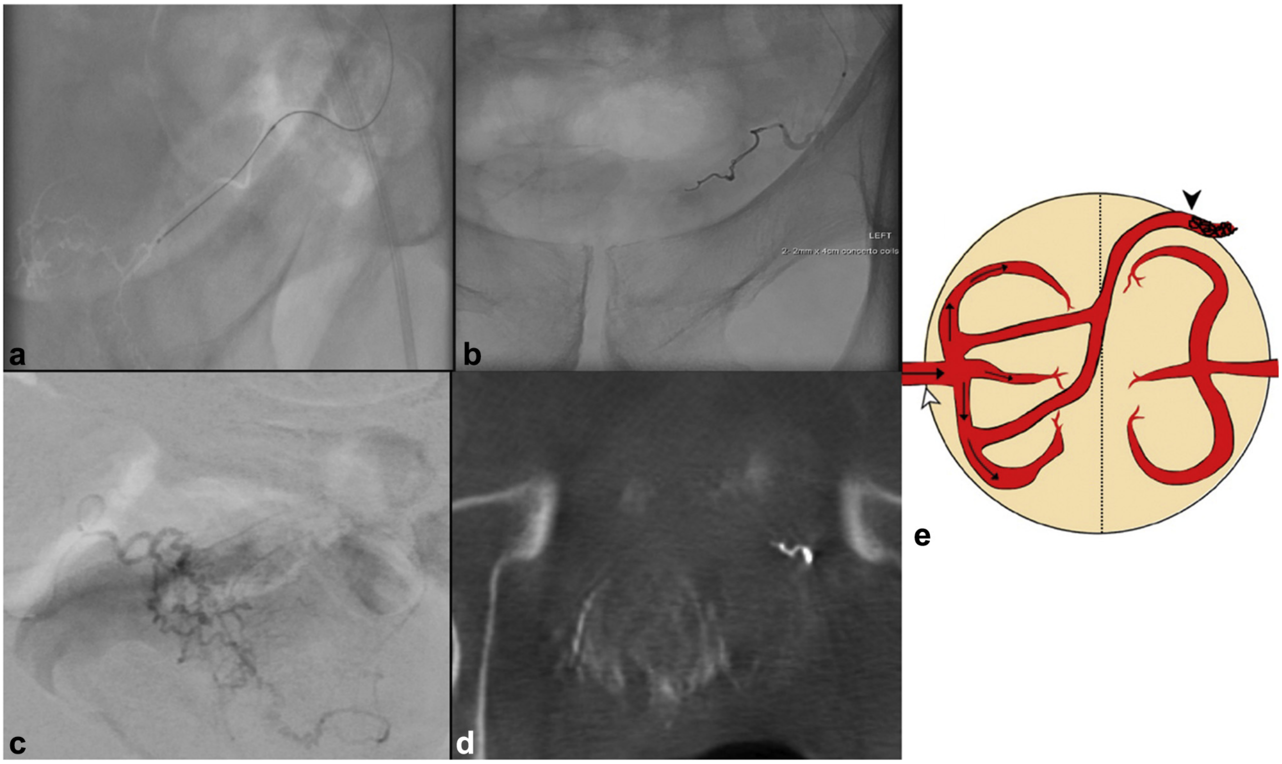

Figure E7. (**a**) Fluoroscopic image with roadmap displaying the position of the catheter in the contralateral left transverse pedicle prior to coil deployment (**b**) Angiography of the left contralateral transverse pedicle after coil embolization with two 2 mm x 4 cm Concerto coils. (**c**) Angiography of the right ipsilateral prostatic artery with anterograde flow after coil embolization of the contralateral left transverse pedicle, prior to right-sided PAE. (**d**) Axial cone-beam CT demonstrating right prostate artery injection confirming staining of the right hemiprostate prior to PAE. Note left-sided previously placed contralateral coil as well as very faint residual staining of the left hemiprostate from immediately prior left-sided PAE. (**e**) Line diagram representation of a Type 2 pattern with contralateral supply after coil embolization. Note the representation of the coils in the contralateral transverse pedicle (black arrow head).

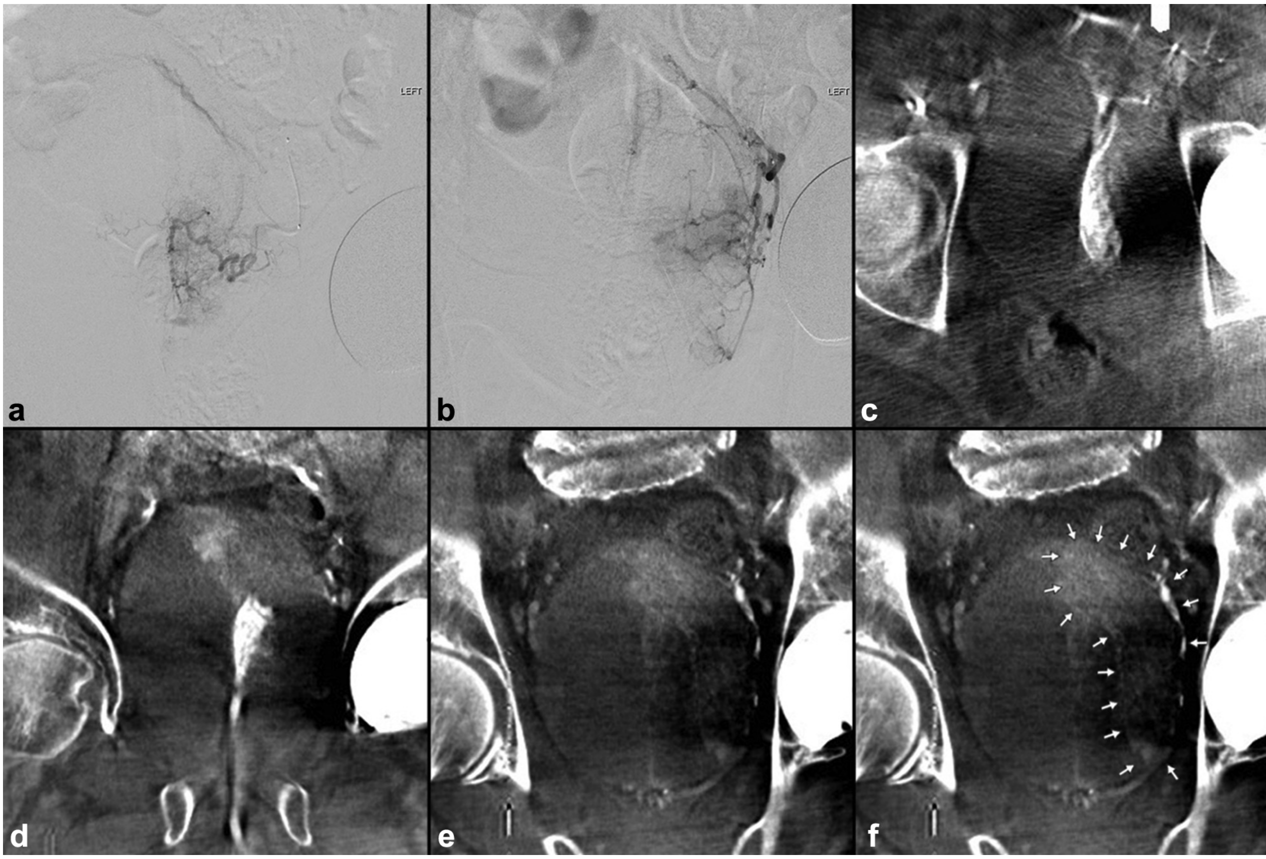

Figure E8. (**a**) Angiography after selective catheterization of the duplicated CG vascular pedicle supplying the medial compartment of the CG. Note the relative large distance of the prostate blush from the medial edge of the left hip prosthesis compared to the lateral pedicle in (**b**). Also note the reduced height of the medial prostate blush relative to the larger-volume lateral glandular blush in (**b**). (**b**) Angiography after selective catheterization and contrast medium injection in the duplicated vascular pedicle supplying the lateral vascular compartment of the CG. Note relative short distance of the lateral prostate blush from the medial edge of the left hip prosthesis compared to the medial pedicle in (**a**). (**c**) Axial cone-beam CT displaying intense opacification of isolated medial vascular compartment after contrast medium injection of the supplying duplicated pedicle. Note extensive artifact in the lateral portion of the left hemiprostate secondary to an artificial hip. (**d**) Coronal cone-beam CT of (**c**). Note that the medial compartment does not involve the entire height of the gland. (height of staining of (**d**) matches height of staining of (**a**) relative to the artificial hip as a reference point). (**e**) Coronal cone-beam CT after injection of contrast medium into the pedicle supplying the superior and lateral vascular compartment after prior embolization of the medial pedicle. Note washout of the medial left CG from immediately prior embolization. Note opacification of the superior and lateral portion of the left hemiprostate, which is subtle due to overlaid artifact from artificial hip (see panel (**f**) for visual aid). (**f**) Duplication of panel (**e**) with arrows outlining the area of opacification of the lateral portion of the left hemiprostate.

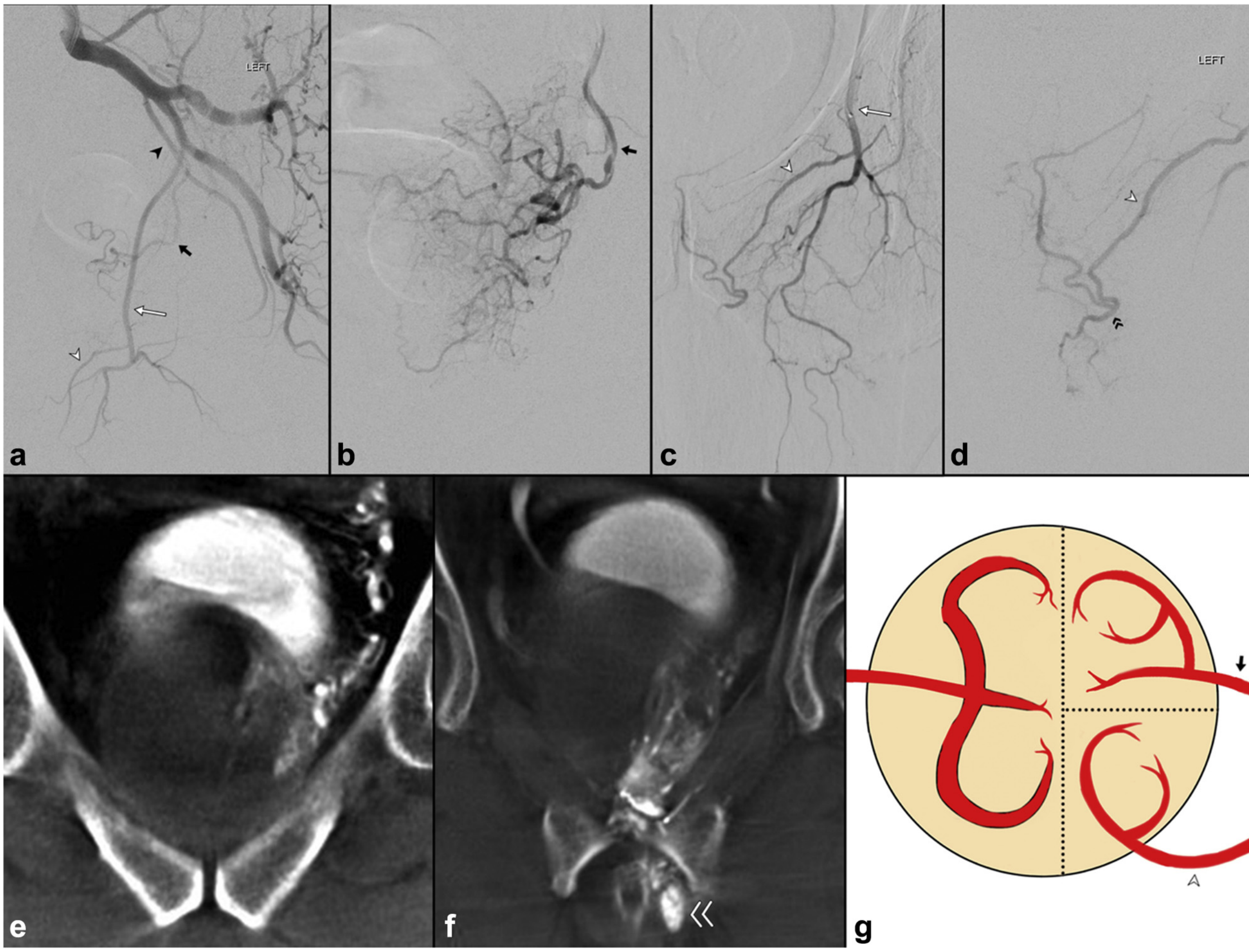

Figure E9. (**a**) Angiography of internal iliac artery. Note IPA (black arrowhead), superior CG pedicle originating from IPA (black arrow), obturator artery (white arrow), and inferior CG pedicle originating from obturator artery (white arrowhead). (**b**) Angiography after selective catheterization of superior CG pedicle originating from IPA (marked by black arrow); a combination of prostatic and vesicular supply was suspected, confirmed on subsequent cone-beam CT. (**c**) Angiography after selective catheterization of obturator artery. Note parent obturator artery (marked by white arrow) and inferior CG pedicle (marked by white arrowhead). (**d**) Angiography after selective catheterization of inferior CG pedicle originating from the obturator artery (marked by white arrowhead). Note a dangerous anastomosis to the corpus cavernosum branches (marked by double black arrow). (**e**) Cone-beam CT after injection of contrast medium in the superior CG pedicle; note opacification in a superolateral distribution of the hemiprostate. Additionally, note the asymmetry of the gland; the right hemiprostate is markedly larger than the left. (**f**) Cone-beam CT after injection of contrast medium in the inferior CG pedicle. Note opacification in an inferomedial distribution reciprocal to the opacification seen in panel (**e**). Additionally, note strong opacification of the left corpus cavernosum (marked by double white arrowheads). (**g**) Line diagram representation of the Type 3 case with separate pedicles supplying reciprocal superolateral and inferomedial compartments with no territorial overlap.

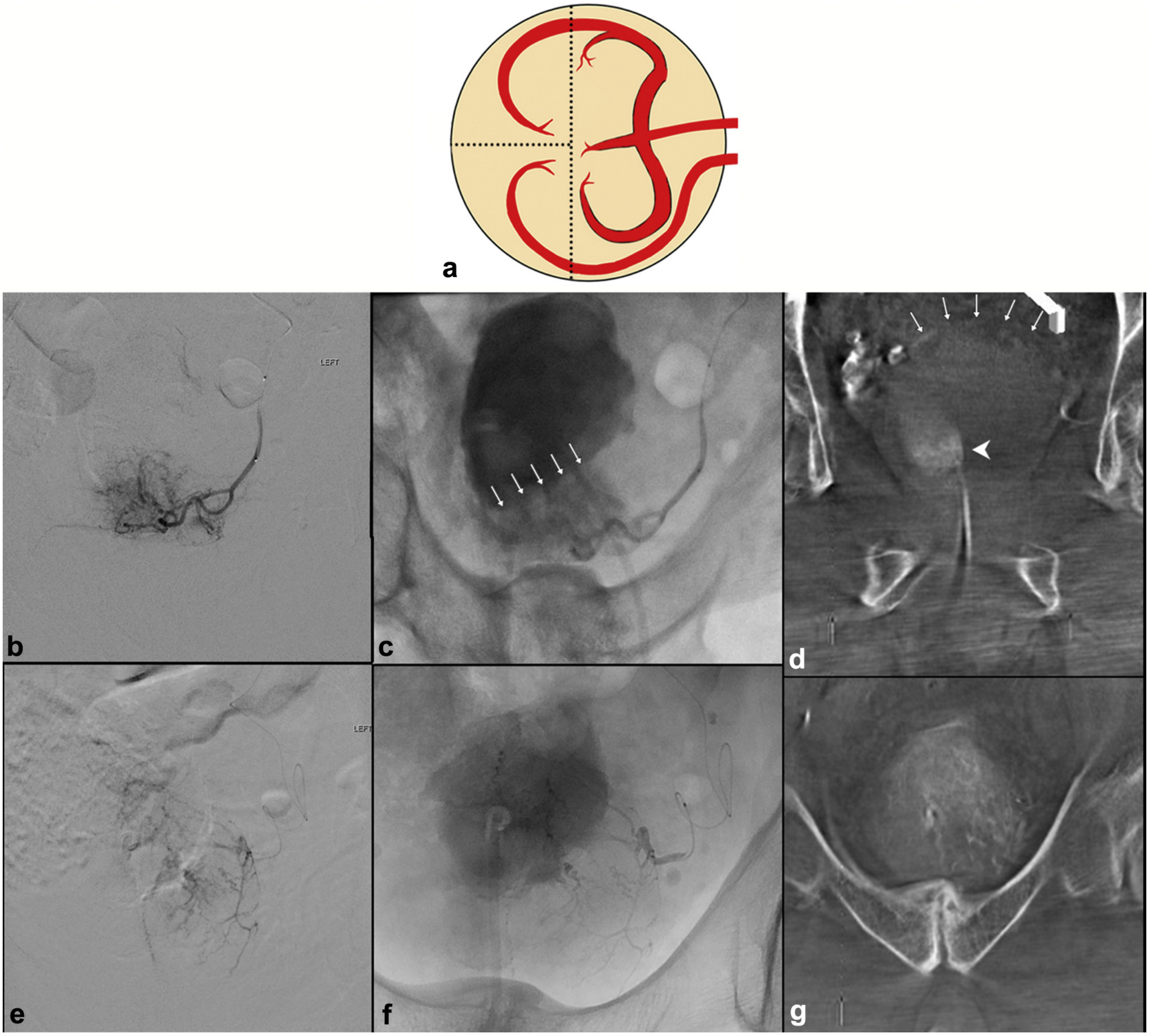

Figure E10. (**a**) Line diagram depicting the Type 3 anatomy and the superior/inferior divide of non-overlapping vascular compartmentalization of the right hemiprostate. (**b**) Angiography of a left CG pedicle originating from the anterior division, feeding the contralateral lower half of the right hemiprostate. (**c**) Unsubtracted angiography of the left CG pedicle feeding the contralateral lower half of the right hemiprostate. Note staining of prostate inferior to opacified bladder. White arrows demarcate the bladder-prostate interface. (**d**) Coronal cone-beam CT after left prostate CG pedicle (**b**) contrast medium injection; note contralateral opacification of the lower half of the right hemiprostate. (**e**) Subtracted angiography of the dominant left prostatic pedicle, feeding the ipsilateral hemiprostate and upper half of the right hemiprostate. (**f**) Unsubtracted angiography of the dominant left prostatic pedicle, supplying the ipsilateral hemiprostate and the upper half of the right hemiprostate. (**g**) Coronal cone-beam CT after dominant prostatic pedicle (**e**) contrast medium injection. Observe ipsilateral left hemiprostate opacification as well as opacification of the right upper half of the contralateral hemiprostate relative to (**c**). Note retention of contrast medium in the lower half of the right hemiprostate from immediately prior PAE.